Extraordinary effects in quasi-periodic gold nano-cavities: enhanced transmission and polarization control of cavity modes

R. Dhama,[†] H. Caglayan,[‡] L. Petti,[¶] A. R. Rashed ,[§] V. Caligiuri,[†] M. Rippa,[¶] R. Lento,[†] R. Termine,[†] and A. De Luca[*,†]

†*Department of Physics, University of Calabria and CNR Nanotec, S.S. di Cosenza, 87036 Rende, (Italy)*

‡*Laboratory of Physics, Tampere University of Technology, 33720, Tampere, (Finland)*

¶*CNR - Institute of Applied Sciences and Intelligent Systems "E. Caianiello", 80072 Pozzuoli, (Italy)*

§*Nanotechnology Research Center, Bilkent University, 06800 Ankara (Turkey)*

E-mail: antonio.deluca@fis.unical.it

Abstract

Plasmonic quasi periodic structures are well known to exhibit several surprising phenomena with respect to their periodic counterparts, due to their long range order and higher rotational symmetry. Thanks to their specific geometrical arrangement, plasmonic quasi-crystals offer unique possibilities in tailoring the coupling and propagation of surface plasmons through their lattice, a scenario in which a plethora of novel phenomena can take place. In this paper we investigate the Extra-Ordinary Transmission (EOT) phenomenon occurring in specifically patterned Thue-Morse nano-cavities, demonstrating noticeable enhanced transmission, directly revealed by near field optical experiments, performed by means of a Scanning Near-field Optical Microscope (SNOM). SNOM further provides an intuitive picture of confined plasmon

modes inside the nano-cavities and confirms that localization of plasmon modes is based on size and depth of nano-cavities, while cross talk between close cavities via propagating plasmons holds the polarization response of patterned quasi-crystals. Our performed numerical simulations are in good agreement with the experimental results. Thus the control on cavity size and incident polarization can be used to alter the intensity and spatial properties of confined cavity modes in such structures, which can be exploited in order to design novel plasmonic device with customized optical properties, desired functionalities and for several applications in quantum plasmonics.

Keywords

Plasmonic quasi-crystals, Nano-cavities, Enhanced transmission, Near-field optical images, Cavity modes

Surface plasmons (SPs) arise from a resonant coupling between incident light and collective oscillations of the conduction electrons present in metallic nanostructures. Their localization and propagation can be engineered by specifically designing plasmonic resonators geometry opening new prospectives in various interdisciplinary fields[1,2]. The observation of very large transmission enhancement through subwavelength periodic metallic nano-holes with respect to theoretical predictions in the framework of Bethe's standard diffraction theory[3], is known as Extra-Ordinary Transmission (EOT)[4,5]. This phenomenon is considered a breakthrough in plasmonics, opening to numerous novel applications. However, despite the fascinating implementations, the physical origin of the enhanced transmission has been extremely controversial and under debate[6,7]. Several theoretical and experimental studies by Ebbesen and co-workers suggest that enhanced transmission appears due to the involvement of propagating and localized SPs[5,8,9]. An alternative interpretation based on a composite diffracted evanescent wave (CDEW) model has been proposed as well[10–12]. According to this model, the detected signal on the output of a structure propagates in the far field due to the interference of surface evanescent waves with the directly transmitted waves passing through the holes and no contribution from SPs is taken into account.

Despite all these controversial points of view, manipulating light matter interaction through metallic nano-apertures enables several applications in plasmonic biosensing[13,14], tunable and selective wavelength filters[5], increased signal in surface enhanced Raman spectroscopy for single molecule detection[15] and near field optics[16,17]. Furthermore, tailoring plasmonic resonances in particularly designed nanoplasmonic devices, SPs have also been exploited as information carriers, thanks to their ability to confine, concentrate and channel light through sub-wavelength structures. This envisages a future where SPs based circuits can be merged with electronics on same chip, in order to offer miniaturized and faster devices[18].

However, it is well known that far-field measurements can not clearly distinguish the role of SPs, due to the bound nature of their electromagnetic field, whose salient features arise in the near field propagating regime. Scanning Near-field Optical Microscopy (SNOM) enables the opportunity to visualize the surface plasmons mediated mechanisms as well as the enhanced transmission phenomenon through particular patterned structures, beyond the diffraction limit[19,20]. When these nano apertures (usually called nanoholes) are patterned in order to exhibit long range order and higher rotational symmetry, but no translational symmetry, are known as quasi crystals (QCs)[21,22]. QCs demonstrate special features with respect their periodic counterparts, such as the ability to create a band gap for low refractive index material[23], a polarization and incident angle independent broad transmission enhancement[24], as well as the possibility to mimic a conventional lens[25] and light harvesting property in solar cells[26]. Till now, optical properties were investigated on such plasmonic structures designed either patterning air holes in metallic films or placing nano-discs in periodic and quasi-periodic arrangements.

Here we report on near and far field spectral properties of quasi-periodic plasmonic nano-cavities (NCs), fabricated by patterning a Thue-Morse (T-M) array of nano-holes in a polymeric film and thermally evaporating a thin gold layer to obtain perfect metallic nano-cavities with gold also inside the holes. Such a quasi-periodic configuration allows unique coupling possibilities between propagating and localized surface plasmons. We demonstrate enhanced transmission through sub-wavelength T-M patterned nano-cavities, as a consequence of the strong coupling

between surface plasmon polaritons (SPPs) and cavity plasmon resonances (CPRs). The presence of gold inside the nano-cavities completely rules out the possibility of an explanation within the framework of the CDEW model, pointing out the plasmonic nature of the EOT phenomenon. SNOM investigations confirm that NCs are the only source of transmitted light via SPPs strong coupling with CPRs in such sub-wavelength quasi-structures. Furthermore, this plasmonic coupling enables polarization and size dependent cavity modes in T-M patterned structures with increased nano-cavities diameter, causing the appearance of surface plasmon pattern waves which reduces the overall EOT effect. In particular, 750 nm diameter T-M structure is able to confine efficient quadrupole modes under crossed polarizers configuration and proper resonant excitation laser source. We also show that dodecagonal quasi-periodic structure preserves the polarization independent response, attributed to the particular arrangement of NCs and cavity-cavity interactions via propagating plasmons.

Results and discussions

T-M patterned structures with different diameters (⌀) as well as a dodecagonal structure, have been fabricated by means of a nano-lithography procedure reported in the Methods section[27–29]. Samples are identified as S-A (⌀=250nm), S-B (⌀=400nm), S-C (⌀=500nm), S-D (⌀=750nm) and S-E (dodecagonal with ⌀=500nm), respectively, (see Figure 1a for details). Scanning electron microscopy (SEM) images of S-B and S-E confirm the fabrication of T-M and dodecagonal quasi-periodic patterns (see Figure 1b and 1c), while uniform presence of gold inside the NC is clearly evident in the inset of Figure 1b. A sketch representing the coupling mechanism between an impinging plane wave (E_i) and a single nano-cavity is reported in Figure 1d. The plane wave impinging on the nano-cavity excites SPPs on both sides of the deposited gold film, at the two interfaces with air (outer) and resist (inner), as well as inside each nano-cavity. Propagating plasmons (SPPs) strongly couple with the specific resonant cavity modes (CPRs), causing the appearance of a confined behavior in near field regime and a propagating one in far-field.

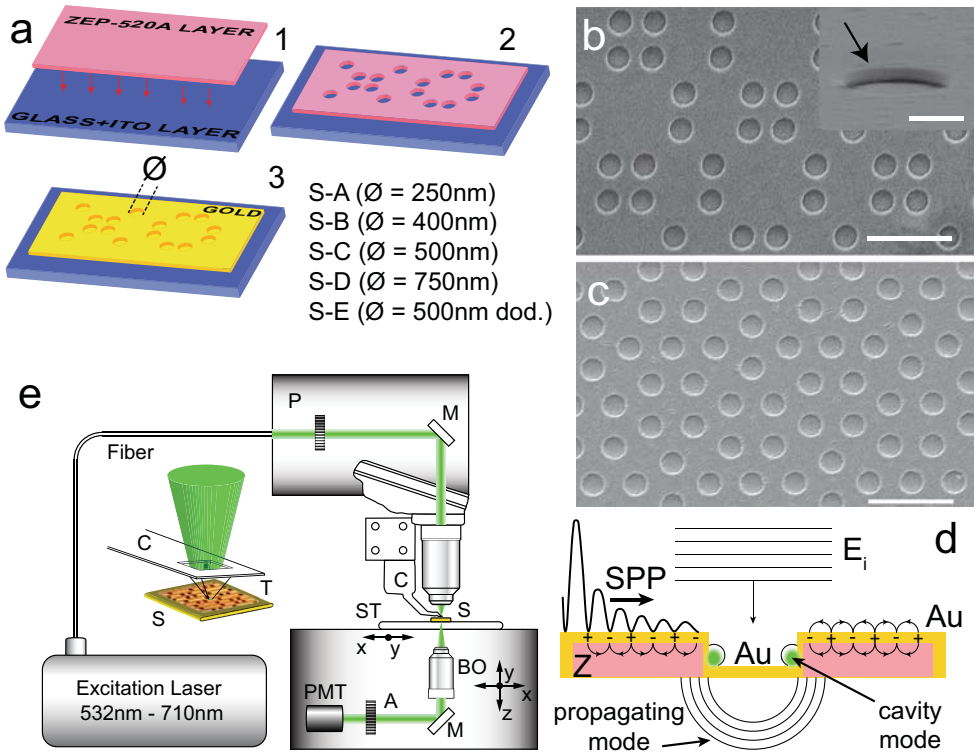

Figure 1: (a) Thue-Morse (T-M) patterned plasmonic nano-cavities with different diameters, ranging from 250nm to 750nm, as well as a dodecagonal array, have been fabricated and named as sample S-A (⊘=250nm), S-B (⊘=400nm), S-C (⊘=500nm), S-D (⊘=750nm) and S-E (dodecagonal array with ⊘=500nm), respectively. (b) SEM image of T-M patterned plasmonic structure sample-B (scale bar of 2μm), while inset shows the depth and deposition of gold inside nano-cavity (Scale bar is of 200 nm). (c) SEM image of dodecagonal quasi periodic pattern sample-E. Scale bar is of 2μm. (d) Sketch of a NC section with an incident plane wave (E_i), the induced SPP that propagates at the inner and outer metal-dielectric interface, and the coupling with the resonant cavity modes (CPRs), to propagate in the far-field. (e) Schematic and beam path of WITec Alpha 300S SNOM for near and far field optical experiments in transmission mode. Inset: particular of the cantiliver and tapered aluminum SNOM tip. P is polarizer, A is analyzer.

Figure 1e reports the schematic and beam path of the SNOM system used to perform near and far field optical experiments in transmission mode.

Optical investigation

To investigate the optical transmittance of the obtained quasi-periodic nano-cavities, a SNOM (Alpha 300S by WITec) has been used in confocal transmission mode. The transmitted signal acquired

from the quasi-periodic structures has been compared and normalized to that one coming from an un-patterned gold film of same thickness, taken as a reference, under the same experimental conditions (incident power and polarization of excitation laser source, $\lambda_{exc} = 532nm$). The laser beam is focused on the samples through a long working distance 100x objective (0.75 numerical aperture (NA)), while transmitted light is collected from the bottom by a 50x objective (0.5 NA) and detected by a photomultiplier tube (PMT). We observe a 3.15-fold and a 2.9-fold enhancement in PMT counts in the case of S-A and S-B with respect to the un-patterned gold film, respectively (see supplementary Figure S1). On the contrary, transmitted signal through S-C, S-D and S-E are comparable with the reference. This surprising enhancement in PMT counts happening only through the two sub-wavelength plasmonic NCs (S-A and S-B) induced us to perform a far field spectroscopic analysis on all the samples. An incident beam coming from an incoherent white light source have been focused on the structures and the transmitted light has been detected in the far field. To demonstrate net transmission enhancement through patterned structures over un-patterned gold film, we defined delta transmission (Δ_T) as:

$$\Delta_T = \frac{I_{T(p)} - I_{T(up)}}{I_{T(up)}} \tag{1}$$

Where, $I_{T(p)}$ and $I_{T(up)}$ represent transmitted intensity through patterned structures and un-patterned gold film, respectively.

This normalized quantity ensures that the common transmitted peak due to d-orbital intraband transitions, which is an intrinsic property of gold, is excluded[19,30]. Figure 2a shows the net enhanced transmission spectra for the five patterned structures, while the inset reports the transmission spectrum of un-patterned gold film, exhibiting the intraband transition peak around 500nm. Sample A exhibits broadband transmission enhancement in the visible range, followed by two maxima at 900nm and 965nm, while sample B presents a maximum around 710nm, and two additional peaks at the same spectral positions of the observed maxima in S-A. In addition, patterned structures also show minima in transmission at specific wavelength regions, which are attributed

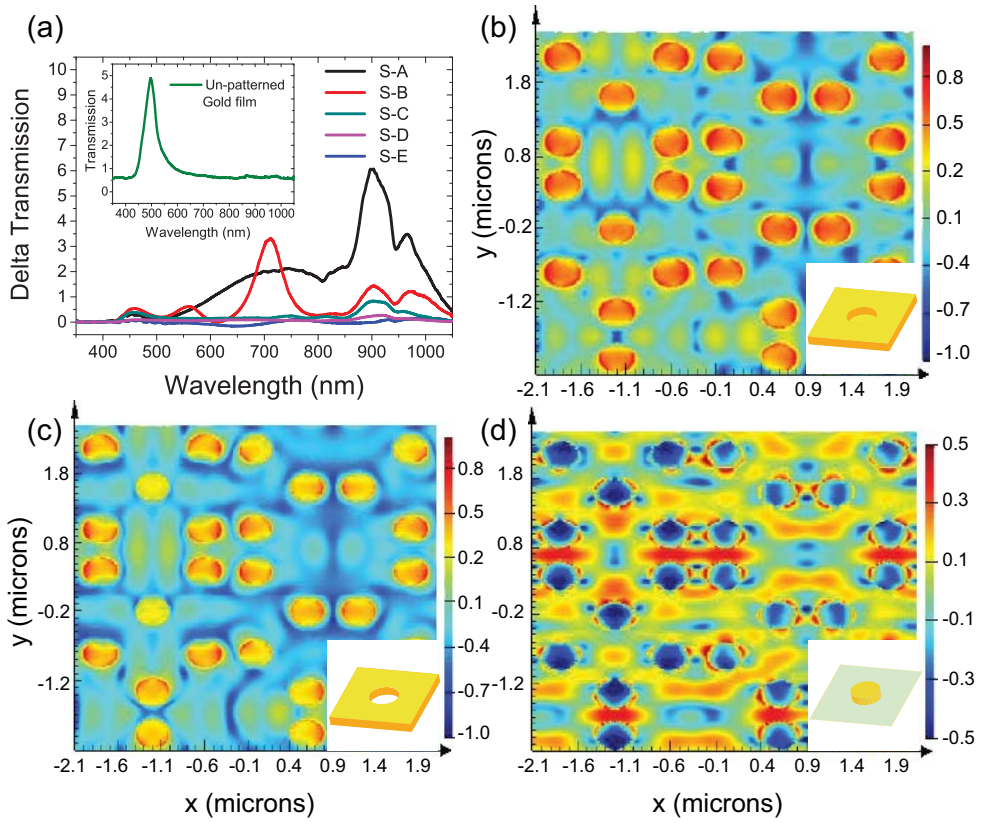

Figure 2: (a) Delta transmission through different sized nano-cavities, while inset shows the transmission through un-patterned gold film. Electric field profiles of sample B and its deconstructed components such as T-M patterned plasmonic nano-cavities (b), nano-holes (c) and nano-discs (d) at the excitation of 710nm incident light, respectively. Insets of figures 2b, c and d are the sketches of a nano-cavity, nano-hole and nano-disc, respectively.

to Wood's anomaly, a phenomenon that occurs when diffracted incident waves become tangent to air/metal interface of patterned films[31]. Enhanced transmission effect reduces as the nano-cavity diameter is increased. In fact S-D transmits almost the same amount of light with respect to the un-patterned gold film as shown in Figure 2a (purple curve).

Moreover, comparison between transmission spectra of S-C (T-M configuration) and S-E (a dodecagonal quasi-periodic pattern) clearly reveal how the rotational symmetry and cavity-cavity interactions also play a role in the transmittance of the structures[32]. S-C shows an enhanced peak around 900 nm, while S-E does not present any transmission enhancement in the whole spectral range (Figure 2a). We attributed the enhanced transmission effect observed in S-A and S-B to the coupling of SPPs, propagating on the both sides of the deposited gold film, with the cavity plasmon

resonances (see sketch in Figure 1d). It is well known that, while increasing the diameter of the nano-holes, their cavity plasmon resonances become broader and weaker.[33,34]. For this reason, even the coupling between propagating surface plasmons and cavity plasmon modes inherent to nano-cavities with larger diameter is weaker, preventing the occurrence of the EOT effect as in the cases of S-C, S-D and S-E, independently on the specific lattice arrangement. Observation of enhanced transmission through both sub-wavelength NCs strongly opposes the CDEW model[10,11], which proposes that constructive and destructive interferences of evanescent waves at metal surface with the fraction of impinging plane waves on the aperture leads to enhanced and suppressed transmission, respectively. Our nano-cavities (due to the presence of gold in the bottom of the hole) do not allow the fraction of impinging wave to take part in such process, underlining the role of plasmonic coupling.

In order to further prove the significant role of propagating and localized plasmons coupling towards transmission enhancement, we performed numerical simulations, based on finite difference time domain (FDTD) method, on three different T-M structures of 400nm diameter. Three scenarios have been theoretically investigated: (i) sample S-B (Figure 2b), (ii) T-M patterned structure made of simple nano-holes without gold inside (Figure 2c) and (iii) T-M patterned gold nano-discs on a dielectric (glass) substrate (Figure 2d). All these structures have been excited by a plane wave at 710 nm, the maximum of transmitted peak experimentally observed in S-B. Our simulations show that the plasmonic NCs are able to confine intense electric field with respect to T-M patterned nano-holes, due to the stronger coupling of propagating plasmons with CPRs, as shown in Figure 2b and 2c, respectively. Figure 2d shows a T-M array of nano-discs simulation exhibiting a weaker local field (see reduced scale bar) due to the absence of metal layer and, consequently, of propagating plasmons to be coupled with disc resonances.

To better understand the physics behind this enhanced transmission mechanism and to investigate localization of electromagnetic fields inside the obtained NCs, SNOM technique represents an essential tool exploiting a sharp optical probe used to detect near field at each NC, in order to obtain super resolution imaging, beating the optical diffraction limit. A linearly polarized laser

beam ($\lambda_{exc} = 532nm$) has been tunnelled through an Al coated aperture SNOM tip, with a diameter of about 60 nm, in order to collect near-field information in transmission mode as shown in the inset of Figure 1e.

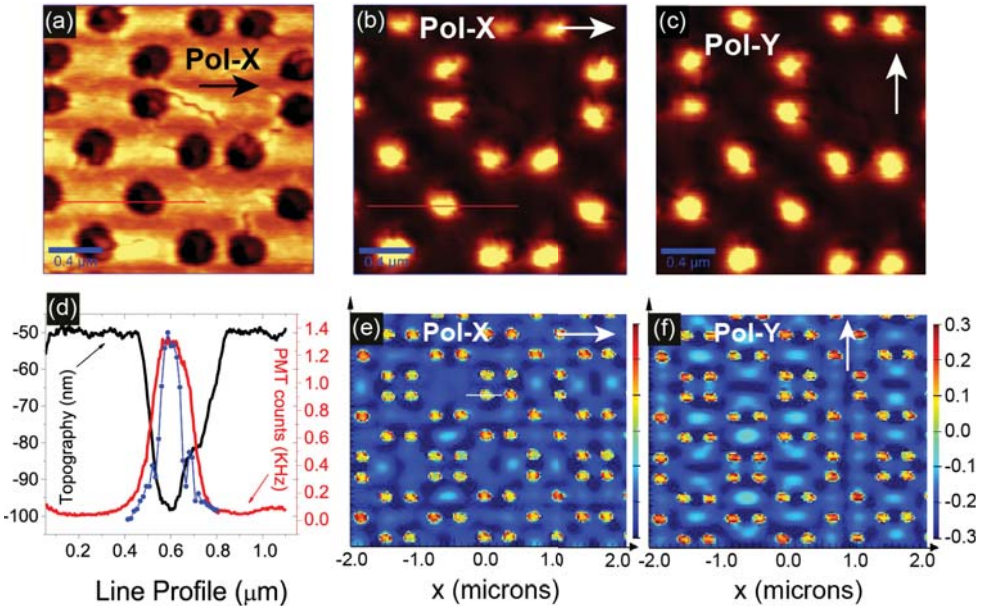

Figure 3: Polarization independent near field response of sample A. (a,b) Topography and corresponding SNOM images of sample A, when excited by X-polarized 532 nm laser beam. (c) SNOM image of sample A, when excited by Y-polarized laser beam. (d) Line profiles of topography and SNOM images along red line from a and b, together with the simulated line profile (blue circles and line) along white line from e. (e,f) Simulated near-field images of sample A for X and Y-polarized 532nm incident light, respectively.

Figure 3 reports the topographic (a) and transmitted optical near field images (b-c) of sub-wavelength sized nano-cavities (S-A), while the direction of incident polarization is indicated by the white arrow. Sample A shows an intense bright mode inside each nano-cavity not affected by the polarization of the excitation beam, reported as bright spots.

Figure 3d reports the profiles of experimental topography (black line) and near-field images (red line) corresponding to lines drawn in Figures 3a and 3b, respectively and the electric field profile of simulated near-field image (blue circle and line) along the white line marked in Figure 3e, confirming that each nano-cavity is able to confine the light exciting bright radiative plasmonic modes.

Topography image of sample S-A is implemented in the FDTD simulation to obtain the near-field at 532nm. Numerical simulations reproduce very well the polarization independent behavior of near-field evolution of bright spots, as shown in Figure 3e and 3f, referred to the two polarizations.

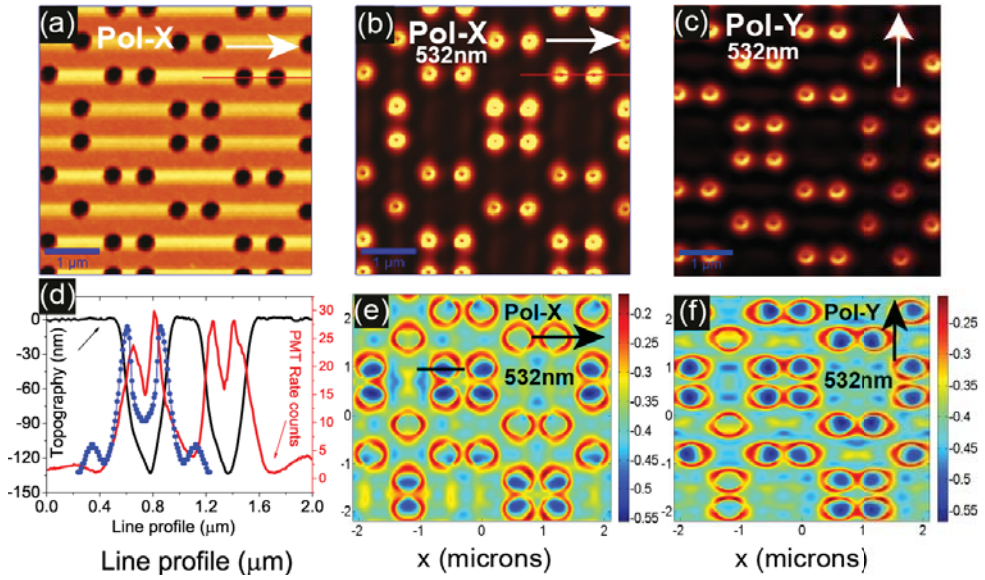

Figure 4: (a,b)Topography and corresponding SNOM images of sample B, when excited by 532nm laser beam with X-polarization. (c) Near field images excited by Y-polarized 532nm laser beam. (d) Line profiles of topography and SNOM images of sample B along red line from (a) and (b), together with the simulated line profile (blue line and circles obtained from black line in (e)). (e,f) Simulated near-field images of sample B for X and Y-polarized 532nm incident light, respectively.

Propagating and localized plasmons coupling mechanism is attributed to the formation of cavity modes in quasi-periodic plsmonic nano-cavities. When incident light through SNOM tip illuminates the thin film based metallic systems, plasmons propagate on the upper and lower metal interfaces due to surface charge distribution on the either side of the film[20,34]. These propagating plasmons become optically active when patterned structure (hole or cavity) offers dipolar localized surface modes along its upper surface[34]. Induced dipole moment along the circumference of cavity and excitations of plasmons on the other side of nano-disc form cavity plasmon resonances (CPRs) in such nano-cavities. Propagating plasmons strongly couple to these CPRs (strong induced dipole moment along the surface of nano-cavity) of S-A and emerge as a bright spot through each NC as shown in Figure 3b and 3c. Gao et al. also imaged enhanced transmission mechanism through

250nm diameter periodic nano-holes drilled in thin gold films and observed the same bright spots across the nano-holes as the first direct evidence of SPPs role in EOT phenomenon[19].

Furthermore, it has been well established (theoretically and experimentally) that the resonances of nano-holes in metallic film are weaker and broader with the increase in hole diameter, very similar to particle resonances[33,34]. Same behaviour is manifested in the case of nano-cavities in thin metallic film and this is what we observed in each nano-cavity of S-B which enables a weaker coupling of propagating plasmons to the cavity resonances. Figure 4b and 4c report the near-field behavior of S-B when excited by means of a X- and Y-polarized laser beam at 532nm, characterized by bright modes on the borders of each nano-cavity and dark spots in the center. Line profiles along the marked red curves of Figure 4a and 4b confirm the presence of donut-type modes in each nano-cavity (see Figure 4d). Figure 4e and 4f report the FDTD simulations obtained for the same sample by starting from the AFM topography images, showing the same donut-type modes. Note, we also performed the same near-field optical experiments on sample B by exciting it at 710 nm, observing bright intense modes instead of such donut-type modes (see supplementary Figure S2). Thus sub-wavelength plasmonic quasi-periodic structures (sample A and B) conclusively show polarization independent near field response and reveal that most of the transmitted signal travels through nano-cavities and emerges as bright and dark spots via different coupling of propagating plasmons to cavity resonances. To further confirm the role of propagating plasmons coupling to localized resonance in the confinement of cavity modes, 400nm diameter T-M nano-discs structure (a deconstructed component of sample B) has been fabricated as sketched in the inset of Figure 2d. Near-field optical experiment on such nano-discs confirms the complete absence of any cavity modes due to the absence of the metal layer used to induce the propagating plasmons in such system (see experimental demonstration in supplementary Figure S3).

Figure 5 demonstrates how even a small increase in cavity diameter modifies both the localization of plasmon modes inside each nano-cavity and the polarization response of the entire system under the same experimental conditions. Figure 5a shows topographic image of S-C, when illuminated by an X-polarized 532nm laser beam. Three intense spots, confined in each cavity as bright

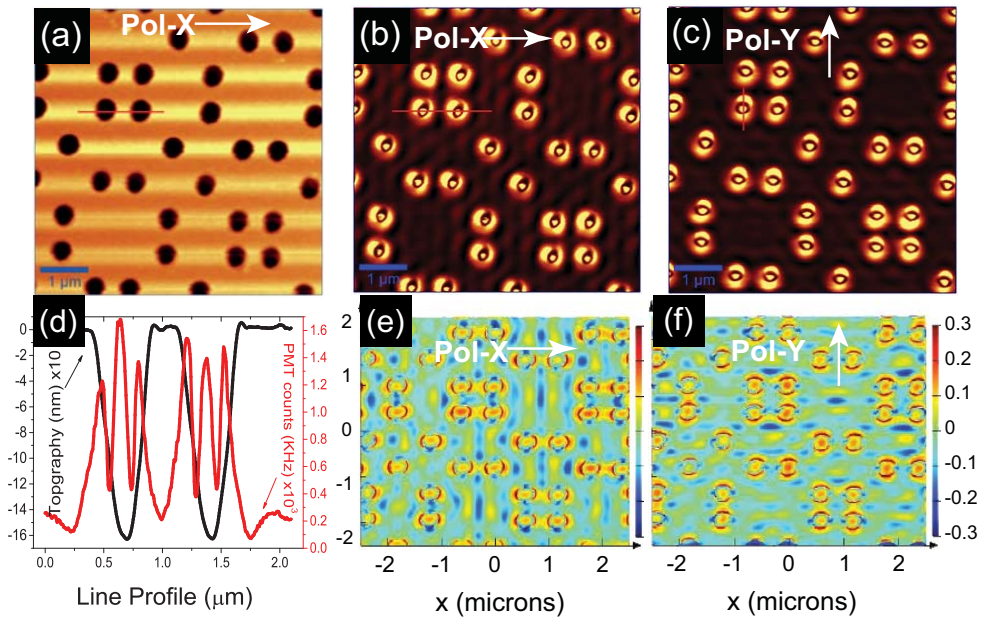

Figure 5: (a-b) Topography and corresponding SNOM images of sample C, when excited by X-polarized 532nm laser beam. (c) Near field image excited by Y-polarized laser beam. (d) Line profiles of topography and SNOM images along red line from (a) and (b). (e-f) Simulated near-field images of the same sample when excited by an X- and Y-polarized light at 532nm, respectively.

modes, are visualized along the polarization direction under excitation (see Figure 5b and 5c). In addition, topographic and near field line profiles of red lines are reported in Figure 5d, clearly confirming the presence of two bright modes coming from the border of the cavity, accompanied by another intense mode located in the center. Simulated near-field images of S-C are in complete agreement with the experiments, confirming the polarization control of the excited modes (see Figure 5e and 5f).

Another effect observed in these quasi-periodic structures is the formation of standing waves on the film surface, more pronounced with the increase in cavity diameter. When propagating plasmons encounter a nano-cavity, they can couple with localized surface plasmon resonances and confine a fraction of their energy inside the NC, while the remaining part is reflected back, causing constructive interference with other propagating plasmon modes and the appearing of intense fringes (standing plasmon polariton waves) on the metallic film[17,35].

In this context, sample A just supports poor fringes due to SPP waves as shown in Figure 3b

and 3c, while fringes originate more clear in S-B, as visualized in Figure 4b and 4c, following the polarization direction of incident light. Furthermore, SNOM images corresponding to S-C demonstrate more intense and numerous fringes (see Figure 5b and 5c) with respect to near field images of S-B in the same traveling distance. Comparison of fringes in near field images of S-B and S-C have been quantitatively reported in *supplementary Figure S4*. Such behavior underlines the fact that strong coupling of propagating plasmons to CPRs of NCs in subwavelength sized T-M structure (sample A and B) allows its major fraction to transmit through cavities in the far field and to reflect a minor fraction utilized in the fringe formation in the near field. On the other hand, weaker coupling takes place with the increase in NCs size (sample C and D) due to weaker and broader CPRs which enhances the scattering nature of cavities irrespective of transmitting via NCs, leading to the formation of strong and intense fringes on the film surface and contributing very few in transmission.

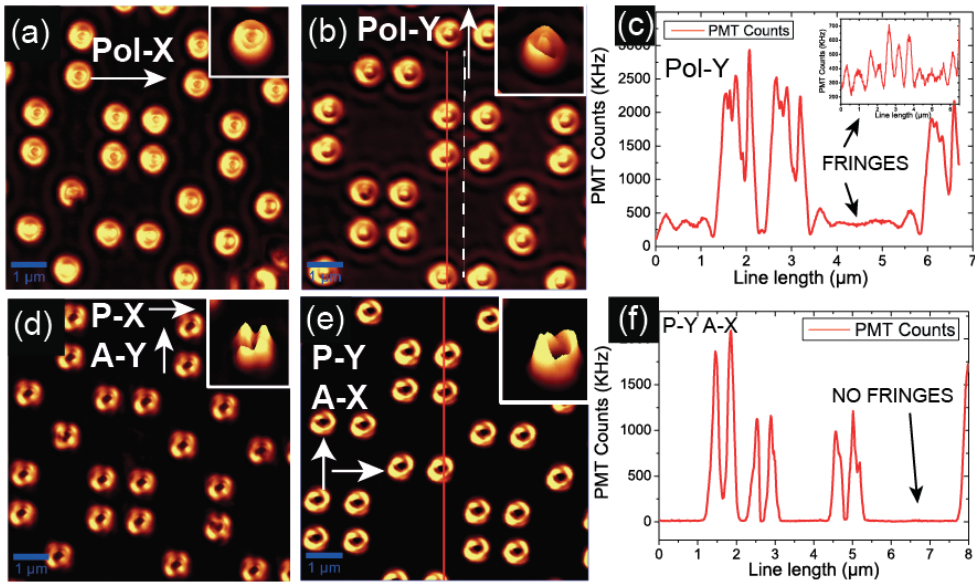

Figure 6: Polarization hypersensitive cavity modes in 750 nm sized T-M nano-cavities named as sample D. (a,b) Corresponding SNOM images of sample D, when excited by X and Y-polarized laser beam, respectively. (c) Line profiles of SNOM images along red line (main graph) and dashed white line (inset), marked through the middle of two nano-cavities in b. (d,e) Rise of quadrupole modes, when polarizations are crossed. (f) Line profile of SNOM image along red line marked in (e), showing no fringe formation. Insets in (a,b,d and e) show cavity modes through one nano-cavity in three dimensional space.

Figure 6 summarizes the extended near field optical experiments performed on sample D, while the insets in all figures show the shape of these cavity modes in three-dimensional space. Plasmon modes confined in such quasi-periodic NCs are referred as Mie-type modes as the radius of cavities lies below the excitation wavelength[36].

In such Mie-type structure, larger size of NCs results in further weaker and broader CPRs. In addition, it also provides an opportunity for SNOM tip to excite plasmons in the larger area inside the nano-cavities and to probe the near-field signal from extremely close distance to the bottom of cavity (disc). We expect that plasmons (localized and propagating) excited on internal side of cavities play much vital role in the confinement of cavity modes in larger sized S-D with respect to propagating plasmons along metallic surface coupled to induced dipole moment along the cavities rim and results in the emergence of polarization hypersensitive cavity modes. Figure 6a displays two ring shaped modes (one ring around the rim of cavity and another inside the NC) as an outcome of plasmonic coupling mechanism in such cavities, when excited by X-pol laser light, while atypical redistribution of electromagnetic fields develops due to the excitation of Y-pol laser beam, as shown in Figure 6b. As it can be seen, the orientation of fringes results along the polarization direction of excitation beam.

Moreover, Kwak et al. demonstrated that by placing a polarizer after the sample and before the detector with a fixed but unknown polarization direction, the orientation of fringe patterns can be changed along the direction of polarization of excitation beam for a 250nm diameter periodic hole array[20]. Here we also placed an analyzer A before the detector (see sketch in Figure 1e). When the polarization direction is crossed with respect to A direction, Mie approximated quasi-periodic structures are able to reproduce well defined quadrupole modes through the NC structures (see Figure 6d and 6e, respectively). Observation of quadrupole modes in the plasmonic structures are of particular relevance to enhance the quality factor of plasmonic cavities[37] and to control the specific plasmon modes of nanowires by manipulating separated nanoantenna's position and shape[38]. Such crossed polarization configuration completely cancel the fringe patterns (standing

plasmon waves) from the near field images. In order to demonstrate this effect, we extracted the intensity of PMT counts along the red lines marked on SNOM images (see curves in Figure 6c and 6f) which have been obtained without and with the analyzer, respectively, while the inset of Figure 6c reports the line profile of a white dashed line as mentioned in Figure 6b in order to visualize the fringes in clearer way.

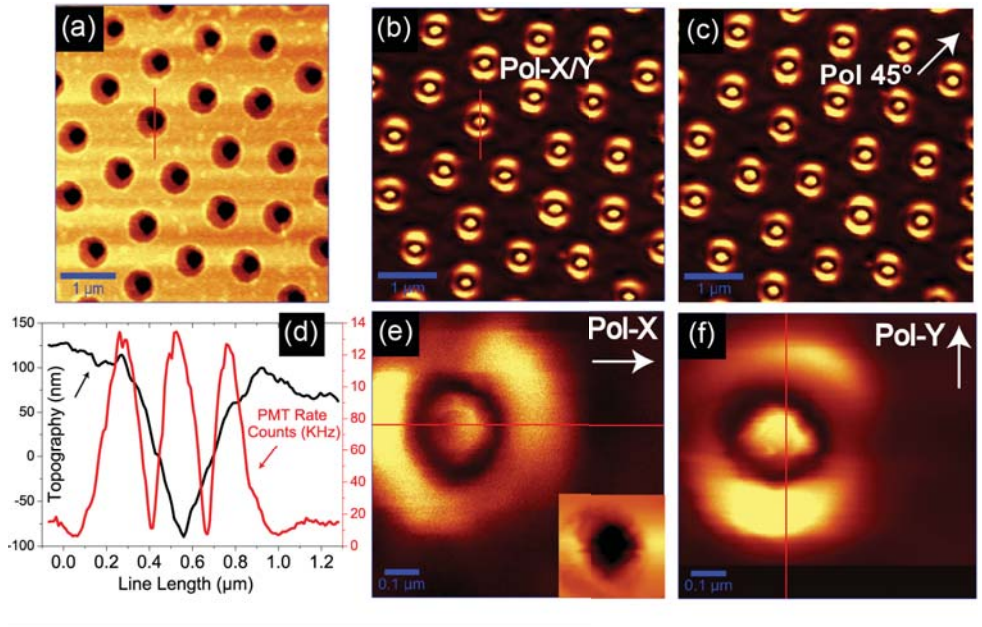

Figure 7: (a) AFM Topography of sample E (500nm diameter dodecagonal plasmonic nano-cavities) (b-c) Polarization independent behavior of the near field localization of light. (d) Line profiles of topography and SNOM images along red line from a and (b). (e-f) Near-field behavior of a single cavity exhibits polarization dependent behavior. Inset in (e) is the AFM topography of the single cavity.

It is well known that polarization insensitivity in nanoplasmonic devices opens up the way towards several applications with different optical functionalities[39,40]. To examine the role of cavity arrangements in the control of optical properties, near-field optical experiments have also been performed on a dodecagonal structure (S-E) patterned by same dimensions (diameter and depth) of nano-cavities of sample S-C in (Figure 5) under the similar experimental condition. Topographic (Figure 7a) and near field images (7b and 7c) clearly show the polarization insensitive response, confining the similar cavity modes obtained in NCs along a specific polarization (X, Y or 45°). In Figure 7d we also report the line profiles of AFM and SNOM images referred to

red lines in Figure 7a and 7b, respectively. Then, we fabricated a single cavity of similar size and depth and investigated its near field response. Figure 7e and 7f report confined modes in the cavity now aligned to the polarization direction of incident light beam, confirming that the near-field polarization independence, observed in the whole sample, depends on specific cavities arrangement and on the interaction between neighbour cavities via propagating plasmons. In the inset of Figure 7e the topographic image of the single cavity is reported.

Conclusion

In conclusion, this work explores how the slight deviations from periodicity and specific plasmons engineering lead to fascinating and unexpected near and far field optical phenomena in quasi-periodic structures. Patterned plasmonic nano-cavities make such quasi-periodic periodic structures very particular and enable the strong coupling between surface plasmon polaritons propagating on the gold surface with the cavity resonances of each nano-cavity. We demonstrated enhanced transmission mechanism via polarization independent near-field responses in the sub-wavelength Thue-Morse arrays of plasmonic nano-cavities. Moreover, the structures with increased nano-cavity diameter demonstrate polarization sensitive nature along with the ability to obtain large field enhancement in terms of cavity modes at precise positions in nano-cavities. Such plasmonic structures can be exploited as substrates in SERS experiments[28], quantum emitters spontaneous emission enhancement, sensing and in the development of polarization sensitive and insensitive next generation photonic devices. We also propose that analytical modeling of plasmon hybridization in such quasi-crystalline nano-cavities can be useful to understand light matter interactions in these complex systems and to unearth several physical phenomena.

Materials and Methods

Fabrication of quasi-periodic plasmonic nano-cavities

180 nm thick layer of electron-sensitive polymer resist, styrene methyl acrylate (ZEP 520A), was spin-coated on 15 nm thick ITO coated glass substrate. Electron beam lithography (EBL) by a Raith 150 was used to nanopattern the holes by following both a T-M and a dodecagonal configuration. In this context, 12.8 pA electron beam with an dose/area of 25 μCcm^{-2} was locally focused on polymer films to expose the particular regions of photoresist and design the quasi-periodic holes structures at 170°C for 5 minutes. Nano-holes were obtained in ZEP layer after developing it in an n-amyl acetate solvent and rinsing for 90s in 1:3 MIBK/IPA solution (methyl isobutyl ketone/isopropyl alcohol), then washed by IPA solution and dried in a gentle flow of argon gas (step 2 of Figure1a). Finally, thermal evaporation of a 60nm thick gold film (evaporating rate of 0.2 s^{-1}) over the quasi-periodic array transforms the nano-holes into uniform plasmonic nano-cavities, (step 3 in Figure 1a). To fabricate 400nm diameter nanodisks, we followed the subsequent protocol. A film of 180 nm thick of ZEP is spin coated on a 15nm ITO coated glass substrate and baked at 170 $^{\circ}C$ for 5 min. The pattern is realized by exposing and developing the sample with the same parameters as for nano-cavities. After these steps, the pattern based on T-M shaped nano-holes with diameter 400nm is generated in the resist film. Deposition of chrome and subsequently gold film having 2nm and 60nm thicknesses, respectively, is made on the sample by using a SISTEC CL-400C e-beam evaporator. After an additional step of gold lift-off accomplished by immersing the sample in Acetone for 20-25 min and then in N-methyl-pyrrolidinone, at 80 $^{\circ}C$, for 5 min the nano-pattern based on gold T-M shaped nano-disks are realized.

Simulations

The calculation of optical properties of the NCs have been performed by means of a finite difference time domain (FDTD) method, implemented with the aid of a commercial software package (Lumerical FDTD Solutions). For the calculation of electric fields, both in near and far field con-

figuration, AFM images have been used in the software, while perfectly matched layer (PML) is used for the boundaries. Gold optical properties have been considered as reported in Johnson and Christy data. The injection of the source is performed in the z direction with a normal incident.

Acknowledgement

The research leading to these results has received support and funding from the Italian Project NanoLase - PRIN 2012, Protocol No. 2012JHFYMC.

Supporting Information Available

Optical transmission of all the quasi-periodic patterned structures and their corresponding unpatterned metal films, as acquired and normalized. Optical behavior of sample B when excited by polarized 710nm laser beam. Optical Investigation of a 400nm T-M stracture of nano-disks. Line profile of sample B and C in the cavity-cavity space, in order to show the presence of standing waves (SPPs) and their relation with the excitation wavelength.

References

(1) Maier, S. *Plasmonics: Fundamentals and Applications: Fundamentals and Applications*; Springer, 2007.

(2) Lal, S.; Link, S.; Halas, N. J. Nano-optics from sensing to waveguiding. *Nat Photon* **2007**, *1*, 641–648.

(3) Bethe, H. A. Theory of Diffraction by Small Holes. *Phys. Rev.* **1944**, *66*, 163–182.

(4) Ebbesen, T. W.; Lezec, H. J.; Ghaemi, H. F.; Thio, T.; Wolff, P. A. Extraordinary optical transmission through sub-wavelength hole arrays. *Nature* **1998**, *391*, 667–669.

(5) Genet, C.; Ebbesen, T. W. Light in tiny holes. *Nature* **2007**, *445*, 39–46.

(6) Visser, T. D. Plasmonics: Surface plasmons at work? *Nat. Phys.* **2006**, *2*, 509–510.

(7) Cao, Q.; Lalanne, P. Negative Role of Surface Plasmons in the Transmission of Metallic Gratings with Very Narrow Slits. *Phys. Rev. Lett.* **2002**, *88*, 057403.

(8) Martín-Moreno, L.; García-Vidal, F. J.; Lezec, H. J.; Pellerin, K. M.; Thio, T.; Pendry, J. B.; Ebbesen, T. W. Theory of Extraordinary Optical Transmission through Subwavelength Hole Arrays. *Phys. Rev. Lett.* **2001**, *86*, 1114–1117.

(9) Barnes, W. L.; Murray, W. A.; Dintinger, J.; Devaux, E.; Ebbesen, T. W. Surface Plasmon Polaritons and Their Role in the Enhanced Transmission of Light through Periodic Arrays of Subwavelength Holes in a Metal Film. *Phys. Rev. Lett.* **2004**, *92*, 107401.

(10) Gay, G.; Alloschery, O.; Viaris de Lesegno, B.; O/'Dwyer, C.; Weiner, J.; Lezec, H. J. The optical response of nanostructured surfaces and the composite diffracted evanescent wave model. *Nat Phys* **2006**, *2*, 262–267.

(11) Lezec, H. J.; Thio, T. Diffracted evanescent wave model for enhanced and suppressed optical transmission through subwavelength hole arrays. *Opt. Express* **2004**, *12*, 3629–3651.

(12) Treacy, M. M. J. Dynamical diffraction explanation of the anomalous transmission of light through metallic gratings. *Phys. Rev. B* **2002**, *66*, 195105.

(13) Sannomiya, T.; Scholder, O.; Jefimovs, K.; Hafner, C.; Dahlin, A. B. Investigation of Plasmon Resonances in Metal Films with Nanohole Arrays for Biosensing Applications. *Small* **2011**, *7*, 1653–1663.

(14) Barik, A.; Otto, L. M.; Yoo, D.; Jose, J.; Johnson, T. W.; Oh, S.-H. Dielectrophoresis-Enhanced Plasmonic Sensing with Gold Nanohole Arrays. *Nano Letters* **2014**, *14*, 2006–2012.

(15) Brolo, A. G.; Arctander, E.; Gordon, R.; Leathem, B.; Kavanagh, K. L. Nanohole-Enhanced Raman Scattering. *Nano Letters* **2004**, *4*, 2015–2018.

(16) Neumann, L.; Pang, Y.; Houyou, A.; Juan, M. L.; Gordon, R.; van Hulst, N. F. Extraordinary Optical Transmission Brightens Near-Field Fiber Probe. *Nano Letters* **2011**, *11*, 355–360.

(17) Yin, L.; Vlasko-Vlasov, V. K.; Rydh, A.; Pearson, J.; Welp, U.; Chang, S.-H.; Gray, S. K.; Schatz, G. C.; Brown, D. B.; Kimball, C. W. Surface plasmons at single nanoholes in Au films. *Applied Physics Letters* **2004**, *85*, 467–469.

(18) Ozbay, E. Plasmonics: Merging Photonics and Electronics at Nanoscale Dimensions. *Science* **2006**, *311*, 189–193.

(19) Gao, H.; Henzie, J.; Odom, T. W. Direct Evidence for Surface Plasmon-Mediated Enhanced Light Transmission through Metallic Nanohole Arrays. *Nano Letters* **2006**, *6*, 2104–2108.

(20) Kwak, E.-S.; Henzie, J.; Chang, S.-H.; Gray, S. K.; Schatz, G. C.; Odom, T. W. Surface Plasmon Standing Waves in Large-Area Subwavelength Hole Arrays. *Nano Letters* **2005**, *5*, 1963–1967.

(21) Vardeny, Z. V.; Nahata, A.; Agrawal, A. Optics of photonic quasicrystals. *Nat Photon* **2013**, *7*, 177–187.

(22) Achanta, V. G. Plasmonic quasicrystals. *Progress in Quantum Electronics* **2015**, *39*, 1 – 23.

(23) Rechtsman, M. C.; Jeong, H.-C.; Chaikin, P. M.; Torquato, S.; Steinhardt, P. J. Optimized Structures for Photonic Quasicrystals. *Phys. Rev. Lett.* **2008**, *101*, 073902.

(24) Kasture, S.; Ravishankar, A. P.; Yallapragada, V. J.; Patil, R.; Valappil, N. V.; Mulay, G.; Achanta, V. G. Plasmonic quasicrystals with broadband transmission enhancement. *Scientific Reports* **2014**, *4*, 5257–.

(25) Huang, F. M.; Kao, T. S.; Fedotov, V. A.; Chen, Y.; Zheludev, N. I. Nanohole Array as a Lens. *Nano Letters* **2008**, *8*, 2469–2472.

(26) Bauer, C.; Giessen, H. Light harvesting enhancement in solar cells with quasicrystalline plasmonic structures. *Opt. Express* **2013**, *21*, A363–A371.

(27) Rippa, M.; Capasso, R.; Mormile, P.; De Nicola, S.; Zanella, M.; Manna, L.; Nenna, G.; Petti, L. Bragg extraction of light in 2D photonic Thue-Morse quasicrystals patterned in active CdSe/CdS nanorod-polymer nanocomposites. *Nanoscale* **2013**, *5*, 331–336.

(28) Rippa, M.; Castagna, R.; Pannico, M.; Musto, P.; Bobeico, E.; Zhou, J.; Petti, L. Plasmonic Nanocavities-based Aperiodic crystal for Protein-Protein Recognition SERS sensors. *Optical Data Processing and Storage* **2017**, *3*, 54.

(29) Petti, L.; Rippa, M.; Zhou, J.; Manna, L.; Zanella, M.; Mormile, P. Novel hybrid organic/inorganic 2D quasiperiodic PC: from diffraction pattern to vertical light extraction. *Nanoscale Research Letters* **2011**, *6*, 371–371.

(30) Bohren, C. F.; Huffman, D. *Absorption and scattering of light by small particles*; Wiley science paperback series; Wiley, 1983.

(31) Ghaemi, H. F.; Thio, T.; Grupp, D. E.; Ebbesen, T. W.; Lezec, H. J. Surface plasmons enhance optical transmission through subwavelength holes. *Phys. Rev. B* **1998**, *58*, 6779–6782.

(32) Wang, Q.-j.; Li, J.-q.; Huang, C.-p.; Zhang, C.; Zhu, Y.-y. Enhanced optical transmission through metal films with rotation-symmetrical hole arrays. *Applied Physics Letters* **2005**, *87*.

(33) Rindzevicius, T.; Alaverdyan, Y.; Sepulveda, B.; Pakizeh, T.; Käll, M.; Hillenbrand, R.; Aizpurua, J.; García de Abajo, F. J. Nanohole plasmons in optically thin gold films. *The Journal of Physical Chemistry C* **2007**, *111*, 1207–1212.

(34) Park, T.-H.; Mirin, N.; Lassiter, J. B.; Nehl, C. L.; Halas, N. J.; Nordlander, P. Optical Properties of a Nanosized Hole in a Thin Metallic Film. *ACS Nano* **2008**, *2*, 25–32.

(35) Hecht, B.; Bielefeldt, H.; Novotny, L.; Inouye, Y.; Pohl, D. W. Local Excitation, Scattering, and Interference of Surface Plasmons. *Phys. Rev. Lett.* **1996**, *77*, 1889–1892.

(36) Lacharmoise, P. D.; Tognalli, N. G.; Goñi, A. R.; Alonso, M. I.; Fainstein, A.; Cole, R. M.; Baumberg, J. J.; Garcia de Abajo, J.; Bartlett, P. N. Imaging optical near fields at metallic nanoscale voids. *Phys. Rev. B* **2008**, *78*, 125410.

(37) Seo, M.-K.; Kwon, S.-H.; Ee, H.-S.; Park, H.-G. Full Three-Dimensional Subwavelength High-Q Surface-Plasmon-Polariton Cavity. *Nano Lett.* **2009**, *9*, 4078–4082.

(38) Day, J. K.; Large, N.; Nordlander, P.; Halas, N. J. Standing Wave Plasmon Modes Interact in an Antenna-Coupled Nanowire. *Nano Lett.* **2015**, *15*, 1324–1330.

(39) Firby, C. J.; Chang, P.; Helmy, A. S.; Elezzabi, A. Y. Magnetoplasmonic Faraday Rotators: Enabling Gigahertz Active Polarization Control for Integrated Plasmonics. *ACS Photonics* **2016**, *3*, 2344–2352.

(40) Jiang, Z. H.; Lin, L.; Ma, D.; Yun, S.; Werner, D. H.; Liu, Z.; Mayer, T. S. Broadband and Wide Field-of-view Plasmonic Metasurface-enabled Waveplates. *Scientific Reports* **2014**, *4*, 7511.

Graphical TOC Entry

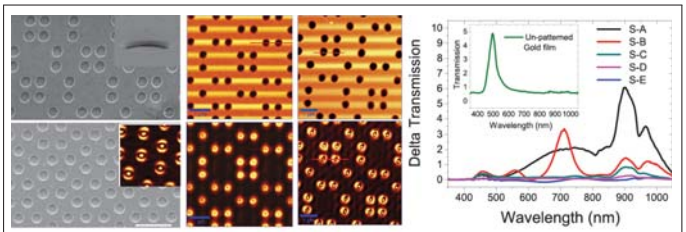

Enhanced transmission and polarization control of cavity modes in quasi-periodic nano-cavities based on Thue-Morse patterns